

A mechanistic study of the $[\text{La}_2(\text{OCH}_3)_2]^{4+}$ - and $[(1,5,9\text{-triazacyclodecane})\text{:Zn}:(\text{OCH}_3)]^+$ -catalyzed methanolysis of carbonates: possible application for the recycling of bisphenol A polycarbonates

Alexei A. Neverov, Leanne D. Chen, Sean George, David Simon, Christopher I. Maxwell, and R. Stan Brown

Abstract: The kinetics of the methanolysis of seven methyl aryl carbonates (**3**) and two methyl alkyl carbonates (**4**) promoted by $[\text{12[ane]N3:Zn}:(\text{OCH}_3)]^+$ and $[\text{La}_2(\text{OCH}_3)_2]^{4+}$ catalysts (**1** and **2**, respectively) have been studied at 25.0 °C. Brønsted plots of the $\log k_2^{\text{obs}}$ values for methanolysis versus aryloxy and alkoxy leaving group (LG) $s_pK_a^{\text{HOAr}}$ or $s_pK_a^{\text{HOR}}$ values (the pK_a values of the parent ArOH or ROH in methanol) for substrates **3** and **4** show an apparent downward break at $s_pK_a \sim 16.6$ and 15.2 with $[\text{12[ane]N3:Zn}:(\text{OCH}_3)]^+$ and $[\text{La}_2(\text{OCH}_3)_2]^{4+}$, respectively. The breakpoint is not due to a change in rate-limiting step in a two-step process involving metal ion delivery of a coordinated methoxide to a transiently associated substrate and the subsequent breakdown of a tetrahedral intermediate to form product. The more satisfactory explanation is that the break arises when one correlates the rate constants for two dissimilar sets of substrates, namely aryloxy- and alkoxy-substituted **3** and **4**. DFT calculations for the **1**-promoted reactions of methyl 4-nitrophenyl carbonate (**3b**), which has a good aryloxy leaving group, and methyl isopropyl carbonate (**4b**), which has a relatively poor alkyl one, indicate that the catalyzed processes involve two steps. Accordingly, the methanolysis of all **3** having $s_pK_a^{\text{HOAr}}$ values for the parent phenols ≤ 15.3 involves rate-limiting nucleophilic attack and fast breakdown. For the isopropyl alkyl derivative (**4b**) having a $s_pK_a^{\text{HOR}} > 18.13$, the rate-limiting step is the metal ion promoted breakdown of a tetrahedral intermediate. The catalytic system employing **2** has utility for the catalytic decomposition of poly(bisphenol A carbonate). In a semi-optimized system where 1000 mg of poly(bisphenol A carbonate), treated at 100 °C for 30 min in 2 mL of 60:40 chloroform–methanol containing $\text{La}(\text{OTf})_3 \cdot \text{NaOMe}$ (5:7.5 mmol L⁻¹), the reaction gave an 84% yield of bisphenol A, corresponding to >300 turnovers per catalyst.

Key words: methanolysis, catalysis, carbonate, polycarbonate, reaction mechanism, DFT computations.

Résumé : On étudie la cinétique de la méthanolyse de sept carbonates de méthylaryle (**3**) et de deux carbonates de méthylalkyle (**4**) favorisée par les catalyseurs $[\text{12[ane]N3:Zn}:(\text{OCH}_3)]^+$ et $[\text{La}_2(\text{OCH}_3)_2]^{4+}$ (**1** et **2** respectivement) à 25,0 °C. Les courbes de Brønsted des valeurs du $\log k_2^{\text{obs}}$ pour la méthanolyse en fonction des valeurs du $s_pK_a^{\text{HOAr}}$ ou du $s_pK_a^{\text{HOR}}$ du groupe partant aryloxy ou alkoxy (les valeurs du pK_a du ArOH ou du ROH parent dans le méthanol) pour les substrats **3** et **4** révèlent une apparente rupture à la baisse aux valeurs de $\sim 16,6$ et 15,2 du s_pK_a avec $[\text{12[ane]N3:Zn}:(\text{OCH}_3)]^+$ et $[\text{La}_2(\text{OCH}_3)_2]^{4+}$, respectivement. Le point de rupture n'est pas attribuable à un changement de l'étape limitant la vitesse dans un processus en deux étapes faisant intervenir la fourniture de l'ion métallique d'un méthoxyde coordonné à un substrat provisoirement associé et la décomposition subséquente d'un intermédiaire tétraédrique pour former le produit. Une explication plus satisfaisante est que la rupture a lieu lorsqu'on établit une corrélation entre les constantes de vitesse de deux ensembles dissemblables de substrats, nommément les composés **3** et **4** contenant des substituants aryloxy et alkoxy. Des calculs par la méthode de la théorie de la fonctionnelle de la densité (DFT) pour les réactions favorisées par **1** du carbonate de méthyl-4 nitrophényle (**3b**), qui possède un bon groupe partant aryloxy, et du carbonate de méthyl-isopropyle (**4b**), dont le groupe partant est relativement mauvais, indiquent que les processus catalysés comprennent deux étapes. Par conséquent, la méthanolyse de tous les dérivés **3** dont les valeurs du $s_pK_a^{\text{HOAr}}$ pour les phénols parents sont $\leq 15,3$ comporte une attaque nucléophile limitant la vitesse et une décomposition rapide. Pour le dérivé isopropyl alkyle (**4b**) dont le $s_pK_a^{\text{HOR}} > 18,13$, l'étape limitant la vitesse est la décomposition de l'intermédiaire tétraédrique favorisée par l'ion métallique. Le système de catalyse faisant intervenir **2** utilise la décomposition catalytique du poly(carbonate de bisphénol A). Dans un système semi-optimisé où 1 000 mg de poly(carbonate de bisphénol A), traités à 100 °C pendant 30 min dans 2 mL d'un mélange 60:40 de chloroforme–méthanol contenant $\text{La}(\text{OTf})_3 \cdot \text{NaOMe}$ (5:7,5 mmol L⁻¹), la réaction a donné du bisphénol A avec un rendement de 84%, ce qui correspond à >300 moles de produit par mole de catalyseur. [Traduit par la Rédaction]

Mots-clés : méthanolyse, catalyse, carbonate, polycarbonate, mécanisme de réaction, calculs DFT.

Introduction

Polycarbonate (PC), such as that made from bisphenol A and phosgene, is widely used in glazing, eyewear, packaging containers, electronics, and optical media (DVD, Blu-ray) and is notable for its impact resistance, clarity, and optical properties. Simple methods for catalytic chemical recycling of these polymers are continually sought, as waste material could be recycled back into

monomer and reused.¹ Existing methods for chemically recycling PC (by methanolysis under basic conditions) typically require pressures of 2–25 MPa, temperature ranges of 75–180 °C, and the presence of stoichiometric amounts of sodium hydroxide or other strongly alkaline catalysts.² These conditions are required, since PC is not soluble in pure methanol under ambient conditions so the surface of the polymer is highly resistant to penetration by

Received 13 June 2013. Accepted 1 August 2013.

A.A. Neverov, L.D. Chen, S. George, D. Simon, C.I. Maxwell, and R.S. Brown. Department of Chemistry, Queen's University, Kingston, ON K7L 3N6, Canada.

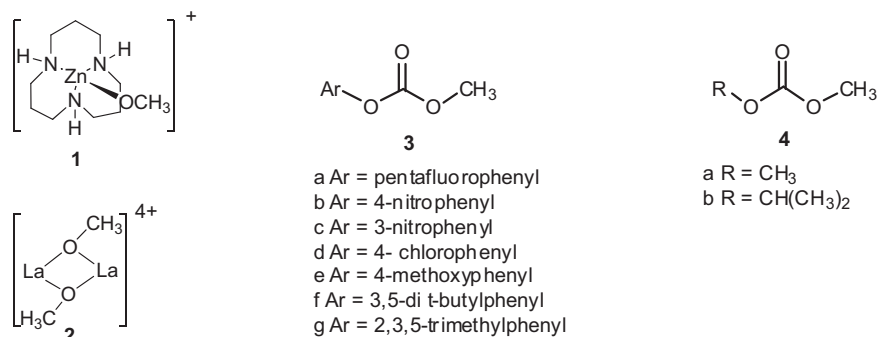
Corresponding author: R. Stan Brown (e-mail: rsbrown@chem.queensu.ca).

solvent and lyoxide. However, two key reports^{3,4} disclosed that methanolysis of PC in the presence of sodium hydroxide at temperatures between 40 and 60 °C is greatly accelerated by surface-softening cosolvents such as toluene, dioxane, chlorinated hydrocarbons, DMF, *N*-methylpyrrolidone, and THF.

Previously, we have reported methods for the metal ion promoted methanolysis of carboxylate⁵ and phosphate⁶ esters where the catalytic systems comprise complexes of certain transition metal ions in methanol as well as lanthanide alkoxides formed in situ. Well studied in these laboratories are (RO⁻):Zn^(II):(1,5,9-triazacyclododecane) complexes (**1**) (which, in methanol, is herein designated as [12[ane]N3:Zn^(II):(OCH₃)]⁺) or simple catalysts containing lanthanide ions such as La^(III), the latter present in solution as a solvated dimeric form with one to five associated methoxides ([La₂(OCH₃)_{*n*}]^{(6-*n*)+}) depending on the 'pH'. Generally, the dimer [La₂(OCH₃)₂]⁴⁺ (**2**) is the most active form exhibiting maximal effect at near neutral conditions of ^spH = 8.8.⁷ These are highly active for promoting transesterification of carboxylate esters, phosphate triesters, and phosphonate diesters in light alcohol solvents such as methanol and ethanol. Attractive features are their ease of preparation in situ, high turnover numbers, large rate enhancements over the

background reactions at neutral ^spH,⁷ and their ability to function at ambient temperature in light alcohols where the metal alkoxides act as both buffers and catalysts. Recently, the use of La^(III) isopropoxide complexed with polyoxy ligands such as 2-(2-methoxyethoxy)ethanol has been shown to have very wide application in the transesterification of esters, carbamates, and dimethyl carbonate,⁸ which underscores the potential utility and wide applicability of these and related catalysts.

Understanding the reaction mechanisms for La^(III) and transition metal ion transesterifications for a variety of substrates is an important step for further development of their utility. The general mechanisms for these catalyzed alcoholyses have been reasonably well established with carboxylate^{5,9} and phosphate/phosphonate esters,^{6,10} so our goal in the current study was (1) to investigate, through kinetic study, the mechanisms for methanolysis of some aryl and alkyl methyl carbonates (**3** and **4**) under ^spH-controlled conditions and (2) to provide DFT-derived computational details for the mechanistic pathway of 1-promoted methanolysis of two selected carbonates (**3b** and **4b**). In addition, we report on some preliminary studies of the La^(III)-containing catalyst that show that it might be suitable for further development into a practical method for the preparative methanolysis of poly(bisphenol A carbonate).



Experimental

Materials

Zn(OTf)₂ (98%), La(OTf)₃ (99.999%), and dimethyl carbonate (99%) were used as supplied (Aldrich) as were dimethylformamide, 1,2-dichloroethane, paraoxon (*O,O*-dimethyl, *O*-(*p*-nitrophenyl) phosphate), sodium methoxide, methanesulfonic acid, trifluoromethanesulfonic acid, ethylene glycol, and paraformaldehyde. Chloroform, tetrahydrofuran, acetone, and dichloromethane were from Fisher Scientific and were used as received. Anhydrous methanol was from EMD Chemicals (DriSolv) and La(OEt)₃ was from Alfa Aesar. PC (poly(bisphenol A carbonate) was obtained from Aldrich as opaque beads (3 mm by 2 mm, batch No. MKAA3883).

4-Nitrophenol (99%), 3-nitrophenol (99%), 4-chlorophenol (99+%), 4-methoxyphenol (99%), 3,5-di-*t*-butylphenol, 2,3,5-trimethylphenol, pyridine (99+%), and methyl chloroformate (99%) were acquired from Aldrich and used as received for syntheses of the corresponding carbonates. Methyl pentafluorophenyl carbonate (97%), methyl phenyl carbonate (97%), and methyl isopropyl carbonate (97%) were purchased from Alfa Aesar.

The other aryl methyl carbonates were prepared following slight modifications of literature procedures.¹¹ In the general procedure, methyl chloroformate was added slowly to the appropriate phenol and pyridine, all in equimolar quantities with methylene chloride as the solvent, and the reaction mixture stirred at room temperature for 12–24 h. Aqueous washings (basic, acidic, neutral) were followed by sodium sulfate drying of the organic layer and evaporation of the solvent. All of the above carbonates

had ¹H NMR and mass spectra consistent with the structure (for physical data for the new carbonates; see the Supplementary material section).

1,5,9-Triazacyclododecane (12[ane]N3) was prepared according to a literature description.¹²

General UV/vis kinetics

Solutions for kinetics were prepared using sodium methoxide (0.5 mol dm⁻³ (Aldrich) or tetrabutylammonium hydroxide (1.0 mol dm⁻³ (Aldrich) and La(OTf)₃ (99.999%), formulating these as stock solutions in anhydrous methanol at 50 mmol dm⁻³. Stock solutions (5 mmol dm⁻³) of each substrate were prepared in 99.8% anhydrous acetonitrile.

Buffer solutions (6.6–20 mmol dm⁻³) were prepared in anhydrous methanol using triethylamine (^spK_a = 10.78),¹³ *N*-ethylmorpholine (^spK_a = 8.6), *N*-methylimidazole (^spK_a = 7.6), and 2,6-lutidine (^spK_a = 6.7) partially neutralized by triflic acid. Reaction solutions were prepared by adding an appropriate amount of the La(OTf)₃ stock solution to a UV cuvette containing buffer so that the total volume was 2.5 mL. The reactions were initiated by the addition of the above substrate stock solutions.

The kinetics of the 2-promoted methanolysis of methyl aryl carbonates **3a–3g** were followed by monitoring the rate of change in absorbance of 5 × 10⁻⁵ to 2 × 10⁻⁴ mol dm⁻³ solutions of each at 274.9, 340, 400, 284, 292, 272, and 272 nm, respectively, using a Cary 100 UV/visible spectrophotometer thermostated at 25 °C. The absorbance versus time data were fit to a standard first-order exponential equation to obtain the first-order rate constants (*k*_{obs})

for the methanolysis of these substrates. The rates of reaction were monitored in duplicate at four to seven different catalyst concentrations from 0.4 to 1.4 mmol dm⁻³. Second-order rate constants (k_2^{obs}) for the catalyzed reactions were obtained from the linear portions of the plots of k_{obs} versus [La(OTf)₃].

For 1-catalyzed reactions, stock solutions of ligand (12[ane]N3), Zn(OTf)₂, and sodium methoxide were prepared in 99.8% anhydrous methanol. A working stock solution was prepared by adding each component in equimolar amounts. This was then diluted in situ with methanol such that the final volume was 2.5 mL in each cuvette. Stock solutions of carbonates 3a–3g were added to initiate reaction and the kinetics of methanolysis were followed by monitoring the rate of change in absorbance of 2.0×10^{-5} to 1.0×10^{-4} mol dm⁻³ of 3a–3g at 258, 320, 330, 284, 291, 272, and 275.9 nm, respectively, as above. The rates of reaction were monitored in duplicate at six different catalyst concentrations from 0.175 to 1.75 mmol dm⁻³. Second-order rate constants k_2^{obs} for the catalyzed reaction were obtained from the linear plots of k_{obs} versus [1].

¹H NMR kinetics

The kinetics of methanolysis of methyl alkyl carbonates 4a and 4b were followed by ¹H NMR spectroscopy (Bruker Avance 500 MHz). Stock solutions of Zn(OTf)₂, La(OTf)₃, and sodium methoxide were prepared in 99.8% deuterated methanol (Cambridge Isotope Laboratories, Inc.). For the 2-catalyzed reactions, the catalytic complex was self-buffered at ^spH = 8.85 in the presence of 0.76 equiv. of methoxide/La³⁺. For the 1-catalyzed reactions, the catalytic complex for each kinetic run was formed in situ through the addition of the Zn(OTf)₂, 12[ane]N3, and sodium methoxide in equimolar amounts. The rate of methanolysis of dimethyl carbonate (4a) was followed by observing the rate of disappearance of the starting materials (CH₃-O-C(=O)-OCH₃, δ = 3.75 ppm) referenced to an acetonitrile standard (CH₃CN, δ = 2.05 ppm) in CD₃OD. The methanolysis of methyl isopropyl carbonate (4b) was followed by observing the rate of appearance of isopropanol ((CH₃)₂CHOH, δ = 1.17 ppm), its concentration being referenced to the acetonitrile standard. The relative integration intensity versus time data were fit to an initial rate expression to obtain the first-order rate constants k_{obs} . The gradients for the k_{obs} versus [1] and k_{obs} versus [2] plots were calculated to give the overall k_2^{obs} .

Methanolysis of PC

Microwave heating was used to heat samples formulated from 200 mg of PC beads crushed to 1–2 mm in size and 2 mL of a chloroform–methanol cosolvent mixture containing La(OTf)₃ and NaOMe (5 and 7.5 mmol dm⁻³, respectively). The weighed polymer samples were placed in 2–5 mL of Biotage microwave vials (rated to withstand a maximum pressure of 20 bar or 2000 kPa) equipped with a magnetic stir bar followed by the addition of cosolvents and stock solutions of the catalyst components. The microwave vial was sealed and placed into a Biotage Initiator Robot Eight microwave oven equipped with a proprietary IR temperature sensor in the microwave cavity. The reaction was set to run for 10 min at 100 °C, this temperature being attained in 30–60 s after the start of the experiment; 1 min after cessation of heating, the temperature was 45 °C, at which time the vial was opened and the contents analyzed. Three different chloroform–methanol cosolvent compositions were subjected to analysis: 50:50, 60:40, and 70:30.

¹H NMR product analysis

The contents of the microwave vial were poured into a small round bottom flask and the solvent removed under vacuum. The crude product was then redissolved in deuterated methanol and analyzed using ¹H NMR spectroscopy. Three different chloroform–methanol cosolvent compositions were subjected to analysis: 50:50, 60:40, and 70:30. In the former case, the residue would not dissolve completely in CD₃OD, indicating incomplete reaction. In

the two latter cases, the residues dissolved completely in CD₃OD and gave ¹H NMR results indicating 97% and 94% reaction completion. Under the reaction conditions described in the Methanolysis of PC section above, homogeneous final solutions in deuterated methanol indicated that the PC had substantially degraded to the point that all of the crude product was soluble in CD₃OD, giving a high conversion of PC to products. The most upfield aromatic hydrogen peak ($\delta \approx 6.69$ ppm) arises from bisphenol A, while the most downfield peak ($\delta \approx 7.2$ ppm) is attributable to unreacted polymer/oligomers. The ratio of the integration of the bisphenol A 6.69 ppm aromatic peak to the sum of the bisphenol A and oligomer peaks at 7.2 ppm was taken as a percentage of reaction completion.

Computational details

Geometry optimizations and free energy calculations of ground- and transition-state structures were completed at the B3LYP level of theory with the IEFPCM¹⁴ methanol solvent model. The 6-31G(d,p) basis set was used for carbon and hydrogen, while 6-31++G(d,p) was used for oxygen and nitrogen. The LANL2DZ¹⁵ pseudopotential was used for Zn(II). Frequency calculations were conducted at this level of theory to characterize stationary points as intermediates or transition states and as a basis for free energy determinations at 298 K. All calculations were conducted using Gaussian 09.¹⁶

Results and discussion

Kinetics

In Fig. 1 is an example of the plot of the k_{obs} for the methanolysis of *p*-nitrophenyl methyl carbonate (3b) as a function of [La(OTf)₃] at ^spH = 8.85. As is observed for the La(III)-catalyzed methanolysis of carboxylate and phosphate esters,^{5,6,17} the plots of k_{obs} versus [La(OTf)₃] at all ^spH values have a significant x -intercept due to the formation of active methoxide-bridged La(III) dimers, [La₂(OCH₃)_{*n*}]^{(6-*n*)+}, where *n* = 1 to 5. The plots are linear above [La(III)]_{total} = 4×10^{-4} mol dm⁻³ where dimer formation is complete in CH₃OH. The gradient of the linear portion of these plots is taken as the second-order rate constant = k_2^{obs} for the La(III)-catalyzed methanolysis of 3 at a given ^spH.

In Fig. 2 is a plot of log k_2^{obs} determined for cleavage of 3b promoted by [La(III) dimers] at various ^spH values; these kinetic data are overlaid with the speciation diagram of [La₂(OCH₃)_{*n*}]^{(6-*n*)+} in methanol that was previously determined by potentiometric titration.¹⁷ The plot has a skewed bell-shape profile maximizing at ^spH ~ 8.8, suggesting that the most active species is the dimer [La(OCH₃)₂]⁴⁺, although [La₂(OCH₃)₃]³⁺ also has good activity that is lessened in accordance with its reduced concentration in solution. Similar experiments were performed for the methanolysis of 3 and 4 promoted by 1 at concentrations between 0.175 and 1.75 mmol dm⁻³; the gradients of the k_{obs} versus [1] plots gave the k_2^{obs} values that are also in Table 1. A representative plot with 3b is shown in Fig. 3.

Brønsted plots

To probe the effect varying the carbonates' leaving groups (LG), we determined the k_2^{obs} values for the 1-catalyzed methanolysis of 3a–3g and 4a and 4b. These constants are given in Table 1 and a Brønsted plot using all data (log k_2^{obs} versus ^spK_a^{HOAr,HOR}) is given in Fig. 4. The black solid and broken lines through the experimental data points for the 1-promoted methanolyses are fits to equations derived from models including all of the data (solid, from treatment of data with equations in ref. 5c), as well as two dashed lines separately treating the aryl carbonates and alkyl carbonates, which appear to fall on two different plots; these will be discussed later. Also given in the figure is a downward breaking red line that describes the Brønsted plot for the k_2^{obs} versus ^spK_a^{HOAr} data for methoxide-promoted methanolysis of 3 determined by Schowen

Fig. 1. Plot of the first-order rate constant for the methanolysis of 4-nitrophenyl methyl carbonate (**3b**) catalyzed by added $\text{La}(\text{OTf})_3$ at $\text{pH} = 8.85$, $T = 25^\circ\text{C}$.

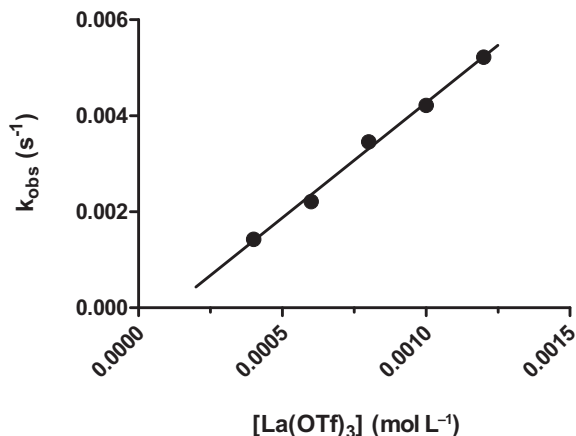


Fig. 2. Plots of the speciation for $\text{La}(\text{III})$ dimers with one to five attached methoxides as a function of pH as computed for $[\text{La}(\text{III})]_{\text{total}} = 2 \times 10^{-3} \text{ mol dm}^{-3}$ from fits of potentiometric titration data.¹⁷ Superimposed on the plots as circles are the k_2^{obs} data for the $\text{La}(\text{III})$ -catalyzed methanolysis of *p*-nitrophenyl methyl carbonate (**3b**) determined at various pH values, $T = 25^\circ\text{C}$.

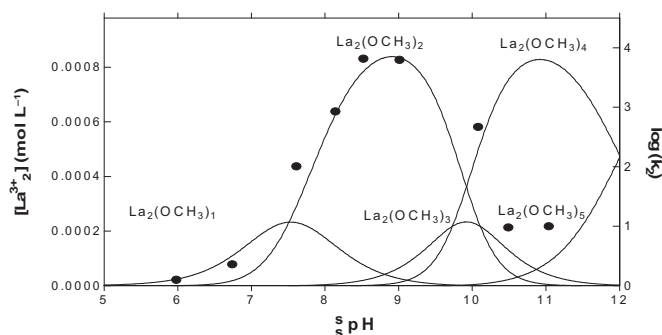


Table 1. Second-order rate constants (k_2^{obs}) for the methanolysis of carbonates **3a–3g** and **4a** and **4b** promoted by **1** and **2** in methanol at $T = 25^\circ\text{C}$.

Carbonate	$\text{pH}_{\text{a}}^{\text{HOAr,HOR}}$	k_2^{obs} for 1 ($\text{dm}^3 \text{ mol}^{-1} \text{ s}^{-1}$)	k_2^{obs} for 2 ($\text{dm}^3 \text{ mol}^{-1} \text{ s}^{-1}$)
3a	8.84	15.83	5.92
3b	11.18	9.42	4.80
3c	12.41	4.92	4.56
3d	13.59	3.38	3.64
3e	14.77	2.86	2.39
3f	14.80	1.87	0.89
3g	15.30	1.09	0.63
4a	18.13	0.05	0.08
4b	19.79	0.001	0.002

Note: k_2^{obs} determined at $\text{pH} = 8.85$ for reactions promoted by **2** and within a pH range of 10.4–11.5 for **1** formed in situ from simultaneous addition of 1:1 $\text{Zn}(\text{OTf})_2$, $12[\text{ane}]N3$, and methoxide.

et al.^{11a} (for a tabulation of these data, see the Supplementary material section).

In Fig. 5 is a similar plot for the methanolysis of **3** and **4** promoted by **2** at $\text{pH} = 8.85$ (corresponding to the pH for maximum activity attributed to catalysis by $[\text{La}(\text{OCH}_3)_2]^{4+}$) (Fig. 2). These constants are given in Table 1 and a Brønsted plot using all data ($\log k_2^{\text{obs}}$ versus $\text{pK}_{\text{a}}^{\text{HOAr,HOR}}$) is given in Fig. 5. The black solid and broken lines through the experimental data points for the

Fig. 3. Plot of the first-order rate constants for the methanolysis of 4-nitrophenyl methyl carbonate (**3b**) as a function of concentration of **1** (formed in situ by addition of equimolar amounts of $\text{Zn}(\text{II})$, methoxide, and ligand, where pH varies from 9.1 to 10.0 with increasing concentration) at $T = 25^\circ\text{C}$.

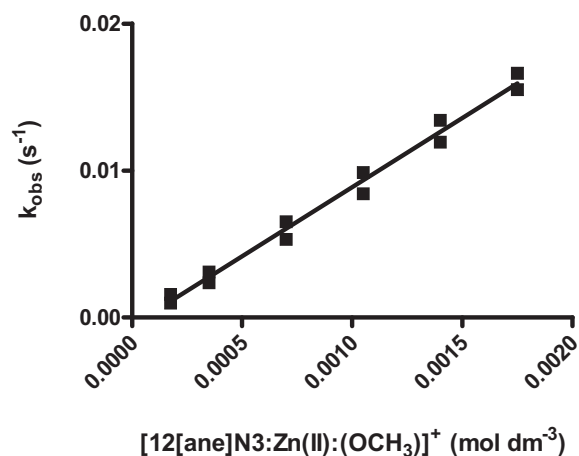
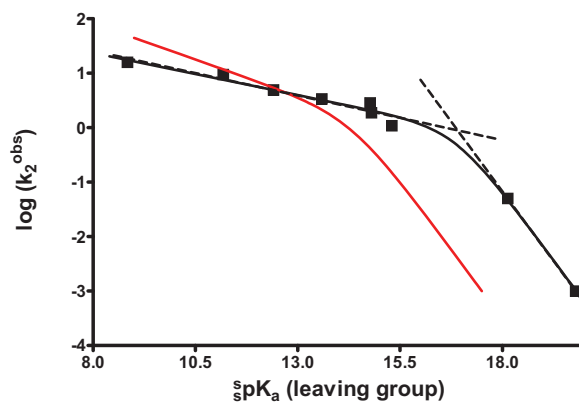


Fig. 4. Brønsted plot of the $\log k_2^{\text{obs}}$ versus $\text{pK}_{\text{a}}^{\text{HOAr,HOR}}$ constants for the **1**-catalyzed methanolysis of carbonates **3a–3g** and **4a** and **4b** determined at $T = 25^\circ\text{C}$. The solid black line through all points was computed from an NLLSQ fit of all of the data as described in ref. 5c, yielding two gradients of -0.15 and -1.02 ; broken lines are the aryl and alkyl carbonates treated separately (**3a–3g** gradient = -0.16 , **4a** and **4b** gradient = -1.0). The red line is the Brønsted plot for methoxide-promoted methanolysis of aryl methyl carbonates was determined by Schowen et al.^{11a}, corrected to $T = 25^\circ\text{C}$ (color in the online version only) (see Supplementary material section).

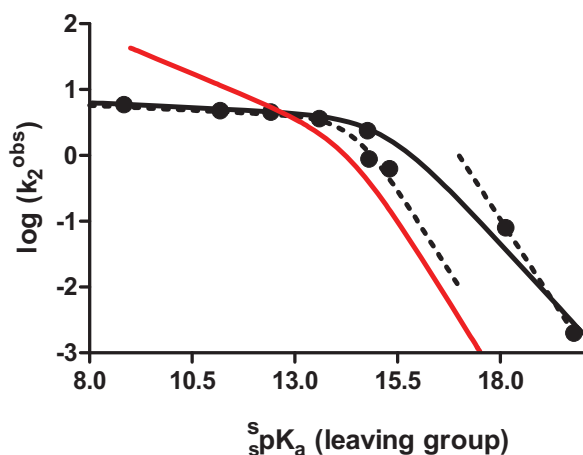


2-promoted methanolyses are fits to equations derived from models^{5c} including all the data (solid), as well as two broken lines separately treating the aryl carbonates and alkyl carbonates, which appear to fall on two different plots; these will be discussed later. The downward breaking red line in Fig. 5 describes the Brønsted plot for Schowen's^{11a} k_2^{obs} versus $\text{pK}_{\text{a}}^{\text{HOAr}}$ data for CH_3O^- -promoted methanolysis of **3** (see the Supplementary material section).

Analysis of the Brønsted plots

The solid black lines through the data in Figs. 4 and 5 exhibit apparent downward breakpoints at $\text{pK}_{\text{a}} \sim 16.6$ and 15.2 for catalysts **1** and **2**, respectively. This behavior was previously observed for metal ion catalyzed methanolysis of aryl and alkyl acetates^{5c} and rationalized at that time as being a result of a change in rate-limiting step from nucleophilic attack on the $\text{C}=\text{O}$ unit of substrates with "good" LG (having lower $\text{pK}_{\text{a}}^{\text{HOAr,HOR}}$ values for their corresponding parent phenols/alcohols) to the departure of

Fig. 5. Brønsted plot of the $\log k_2^{\text{obs}}$ versus ${}^s\text{p}K_{\text{a}}^{\text{HOAr,HOR}}$ for the $[\text{La}(\text{OCH}_3)_2]^{4+}$ -catalyzed methanolysis of carbonates **3a–3g**, and **4a** and **b** determined at ${}^s\text{pH} = 8.85$, $T = 25^\circ\text{C}$. The solid black line is the fit of all data as described in ref. 5c, yielding gradients of -0.03 and -0.68 ; broken lines are the aryl and alkyl carbonates treated separately (**3a–3g** gradients = -0.26 and -1.0 , **4a** and **4b** gradient = -0.97). The red line is the Brønsted plot for methoxide-promoted methanolysis of aryl methyl carbonates determined by Schowen et al.^{11a} (color in the online version only) (see Supplementary material section).



the LG in the case of substrates with the “poor” LG’s (higher ${}^s\text{p}K_{\text{a}}^{\text{HOR}}$ values).

The solid black curved lines in the two figures can each be mathematically deconvoluted^{5c} to provide gradients of -0.15 and -1.02 with a breakpoint at ${}^s\text{p}K_{\text{a}} \sim 16.6$ for the plot in Fig. 4 and gradients of -0.03 and -0.68 with a breakpoint at ${}^s\text{p}K_{\text{a}} \sim 15.2$ in Fig. 5. For both plots, the numerically small gradient in the region corresponding to the methanolysis of the aryloxy carbonates is rationalized as resulting from a cancellation of the electronic effects on substrate binding to the catalysts followed by a rate-limiting nucleophilic attack within the catalyst–substrate complex. Substrates with electron-withdrawing OAr groups will bind to the catalyst more poorly but suffer nucleophilic attack more rapidly, and vice versa. This is similar to the acid-catalyzed hydrolysis of esters where the relative insensitivity of the catalytic rate constant to substitution on the ester was rationalized¹⁸ as a counterbalancing of the alkoxy/aryloxy substituent’s electronic effect on equilibrium protonation and the subsequent nucleophilic addition of water to $\text{C}=\text{O}-\text{H}^+$.

In neither of the Figs. 4 and 5 plots does the breakpoint come at a ${}^s\text{p}K_{\text{a}}^{\text{HOAr,HOR}}$ corresponding to a quasi-symmetrical point where there is a transition between rate-limiting attack to form a tetrahedral intermediate and rate-limiting breakdown of the intermediate. That point should occur where the incoming nucleophile and outgoing LG have identical ${}^s\text{p}K_{\text{a}}^{\text{HOAr,HOR}}$ values. Although it is not clear what these ${}^s\text{p}K_{\text{a}}$ values should be in a metal ion catalyzed process, one can suggest about 9.1 if the reaction is considered to involve a fully metal ion coordinated methoxide as in **1** and 8.1 if it involves $[\text{La}_2(\text{OCH}_3)_2]^{4+}$.¹⁹ Alternatively, if the nucleophile is considered to be methoxide, the quasi-symmetrical point should be at 18.13, the ${}^s\text{p}K_{\text{a}}^{\text{HOCH}_3}$.

We have considered other explanations for breaks in the Brønsted plots that do not result from changes in rate-limiting step^{20,21,22} for the behavior exhibited here. There are interesting cases where members of a set of substrates follow the same general two-step mechanism with rate-limiting attack, but small changes in the substrate may reduce the stability of the addition intermediate to the point it becomes too unstable to exist, immediately decomposing without barrier to product. This sort of

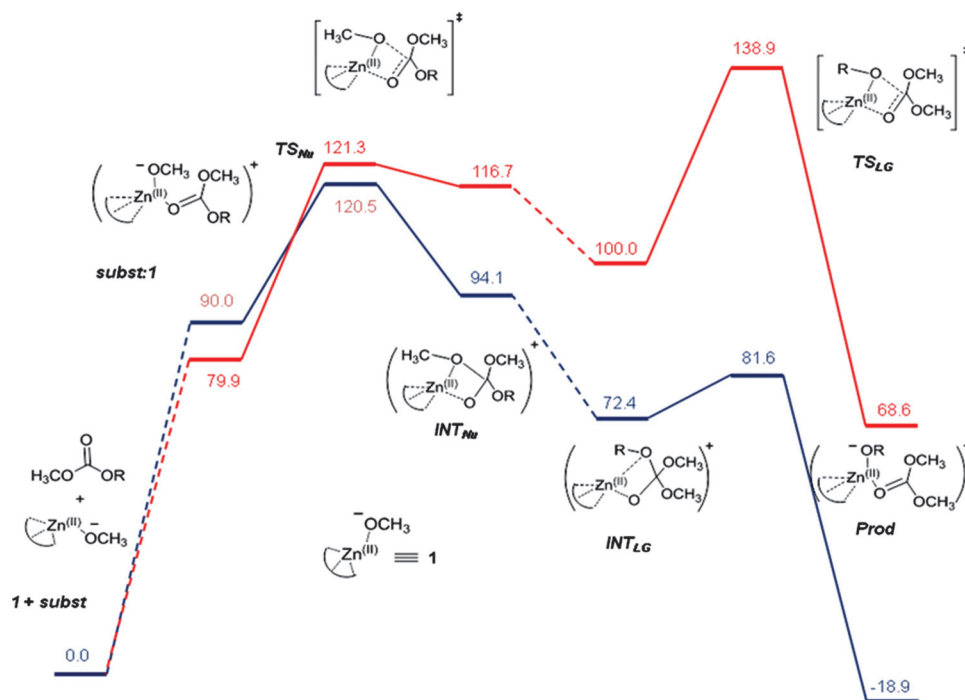
“enforced concerted process”^{23,24} has been recently offered to explain the downward break noted for the $-\text{OH}$ -promoted hydrolyses of a series of aryl-substituted benzene sulphonates.²⁵ Here, it is suggested that substrates with LG having a $\text{p}K_{\text{a}} > 8.5$ proceed via a stepwise process with a pentacoordinate intermediate, while those having a $\text{p}K_{\text{a}} < 8.5$ proceed through a pentacoordinate transition structure but the intermediate produced is too unstable to exist, so the reaction becomes concerted. A recent study of the $-\text{OH}$ -catalyzed hydrolysis of 10 phenyl aryl carbonates ($\text{p}K_{\text{a}}^{\text{HOAr}}$ in water from 5.42 to 9.95) concludes that the reactions are concerted or enforced concerted, with little cleavage of the departing group in the rate-limiting transition state;²⁶ this is also suggested²⁷ to be the case for the ethoxide-promoted ethanolysis of some phenyl aryl carbonates.

Breaks in linear free energy relationships are reported for the methoxide-promoted cleavages of carbonates and acetates with aryloxy LG.¹¹ Given as the red solid lines in Figs. 4 and 5 is the Brønsted plot of the extant^{11a} $k_2^{\text{OCH}_3}$ data for aryl carbonates, which exhibit a downward break at ${}^s\text{p}K_{\text{a}} \sim 14.1$, far lower than the expected quasi-symmetrical point of the conjugate acid of the attacking methoxide (${}^s\text{p}K_{\text{a}}$ methanol 18.13). Schowen^{11a} noted that methoxide attacks on aryl acetates and carbonates are two-step reactions with a rate-limiting addition that becomes progressively less sensitive to the substituent as its electron-withdrawing power increases. Such curvature is not related to a change in rate-limiting step but rather to substrate variations that introduce curvature into a linear free energy relationship, which compares the ΔG^\ddagger of a kinetic process with the equilibrium ΔG° of an acid dissociation process. The nonlinear behavior results from greater importance of the resonance interaction in the equilibrium ionization processes on which the ${}^s\text{p}K_{\text{a}}$ values are based than in the kinetic processes where there is less charge development on the aryloxy group during the nucleophilic attack step.

We have recently addressed the question of breaks in the Brønsted plots for the methanolysis of aryl and alkyl acetates promoted by methoxide and complex **1** with DFT computations and found that there are separate relationships for the aryl and alkyl acetates⁹ that are relevant to the methoxide- and **1**-promoted methanolyses of **3a–3g** and **4a** and **4b**. The reactions catalyzed by **1** involve two steps with a Zn^{II} -coordinated tetrahedral intermediate with all aryloxy acetates except those with the best LG such as 2,4-dinitrophenoxy, where the reaction is concerted or enforced concerted. With a slightly poorer *p*-nitrophenoxy LG, the rate-limiting step is attack, and the departure of the LG is fast, occurring without metal ion assistance. But departure of even poorer aryloxy LG does require assistance of the metal ion, although the reactions of all substrates containing these LG still have rate-limiting attack. With alkoxy acetates, the transesterifications have two steps with metal ion assistance of LG departure, but the latter is rate-limiting only for examples where the LG is worse than methoxide. This work⁹ and our results on the methoxide- and hydroxide-promoted cleavages of aryl and alkyl phosphates and phosphorothioate triesters¹⁰ suggest that downward breaks in their corresponding Brønsted plots arise from the incorporation of members (aryloxides and alkoxides) that adhere to separate lines. In the case of carbonates, the available evidence is consistent with a similar conclusion, but there are only two experimental examples for the metal ion catalyzed processes, which weakens the argument.

Based on the above, we individually evaluate the experimental data for aryl- and alkyl-containing carbonates in Figs. 4 and 5 (broken lines). The data in Fig. 5 for cleavage of **3** promoted by **2** exhibit a small break at ${}^s\text{p}K_{\text{a}} \sim 14.2$, similar to what is observed with the methoxide cleavage of series **3**^{11a} and are displaced from the data obtained for **4**, which form a (two-point) linear free energy relationship unrelated to that obtained with **3**. The reasons for this are not clear, as we were not able to probe this more

Fig. 6. DFT-calculated low-energy pathway for the 1-catalyzed methanolysis of carbonates **3b** (blue) and **4b** (red); free-energy values are reported in kJ mol^{-1} and at 298 K and the diagram is to scale (color in the online version only).



complicated system using DFT calculations.²⁸ In the case of the 1-promoted methanolysis (Fig. 4), substrates **3** are fit satisfactorily with a linear plot, perhaps with the slightest hint of a break at the highest $s_pK_a^{\text{HOAr}}$ values (although the linear relationship fits just as well) and a two-point line for substrates **4** with a steeper gradient of -1.0 . The steeper gradient in the two-point line for **4** could be indicative of a greater charge accruing to the departing alkoxide group but may also be affected by a greater steric demand of the isopropyl group in **4b**. The experimental data do not indicate whether the metal ion catalyzed reactions are concerted or step-wise or, if the latter is the case, whether the metal ion assists in both the attack step and LG departure. Further information is provided by the computational study given below.

Density functional theory study

The mechanisms of the 1-catalyzed methanolysis of substrates **3b** and **4b** were modeled using DFT calculations. The calculated initial binding processes are quite endergonic, although the computed free energy of binding can be considered an overestimation due to an exaggeration of translational and rotational entropic contributions²⁹ and solvation of the ionic species, which is different in the presence of bound substrate. The free energy values for the various reaction intermediates and transition states are reported graphically in Fig. 6 relative to the computed ground states for **1** plus **3b** and **1** plus **4b**. The resulting complexes, **1:3b** and **1:4b**, are trigonal bipyramidal at Zn^{II} with methoxide and two ligand nitrogens occupying the equatorial positions and the carbonate substrate and remaining ligand nitrogen occupying the axial positions. Nucleophilic attack occurs through an attack of the Zn^{II} -coordinated methoxide oxygen on the carbonate carbon (TS_{Nu}) and is associated with a free energy barrier of $120.5 \text{ kJ mol}^{-1}$ for **3b** and $121.3 \text{ kJ mol}^{-1}$ for **4b**. The nucleophilic attack leads to a tetrahedral intermediate INT_{Nu} bound to the metal ion through methoxide and the oxyanion. LG departure was modeled in two ways, with and without metal ion assistance. The free energy barrier for LG departure without metal ion assistance was modeled as a lengthening of the carbonate carbon–LG oxygen bond of INT_{Nu} and is associated with a small barrier ($102.6 \text{ kJ mol}^{-1}$) for **3b**,

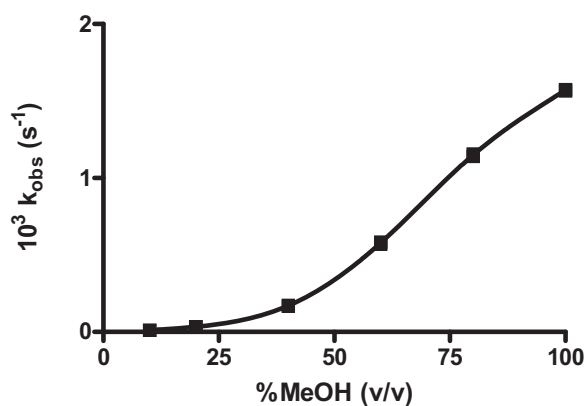
containing a good LG, and a much larger barrier for reaction of **4b** ($197.1 \text{ kJ mol}^{-1}$), which contains the poor LG. To engender metal ion assisted LG departure, a rearrangement must occur in which the nucleophilic methoxide dissociates from the metal ion and the LG is placed in a position where its departure can be facilitated by Zn^{II} . A single transition state for this process could not be found for either **3b** or **4b**; however, potential energy scans indicate that there is only a small (less than $\sim 4 \text{ kJ mol}^{-1}$) barrier for this process. The intermediate prior to metal-assisted departure (INT_{LG}) involves the LG oxygen not bound to the metal but situated 3.22 \AA (**3b**) or 3.05 \AA (**4b**) from it. As the C–O(LG) bond length increases, the Zn^{II} –O(LG) distance decreases such that in the transition state (TS_{LG}), it is 1.70 \AA (**3b**) or 1.80 \AA (**4b**). The free energy barrier for metal-assisted LG departure is lower and not rate-limiting for **3b**, but it is much higher for the alkyl substrate and this transition state represents the rate-determining step for the methanolysis of **4b**. The nucleophilic attack step, TS_{Nu} , is limiting for the substrate with the good LG, **3b**.

Calculations of the reaction free energies for **1** plus **3g** (not shown) having the poorest aryloxy LG indicated the rate-limiting step for this process was nucleophilic addition, with the departure of the LG being metal ion assisted, with a $5\text{--}7 \text{ kJ mol}^{-1}$ lower energy than the attack step. In view of this finding, **3g** is considered to lie on the broken line linear relationship in Fig. 4. The apparent break in the Brønsted relationship in Fig. 5 with the La^{III} -based catalyst, suggesting that **3h** and **3g** might be experiencing a change in rate-limiting step from attack to LG departure, still remains a possibility, but we could not probe this using DFT calculations.²⁹

Catalytic methanolysis of poly(bisphenol A carbonate) (PC)

The initial catalytic system used for the depolymerisation of PC was formulated in methanol adding $\text{La}(\text{OTf})_3$ and NaOMe (5 and 7.5 mmol dm^{-3}). Three beads of commercial PC ($\sim 53 \text{ mg}$) were heated to $100 \text{ }^\circ\text{C}$ in 2 mL of catalyst solution for 10 min with no observable changes to the beads. To determine whether the problem was due to poor catalytic activity or the catalyst transport into the solid PC, the beads were ground and sieved to a particle size of

Fig. 7. Plot of pseudo-first-order rate constants for the methanolysis of **1e** catalyzed by 1 mmol dm⁻³ La(OTf)₃ in the presence of 1.5 mmol dm⁻³ NaOMe as a function of chloroform–methanol solvent composition, *T* = 25 °C. The line through the data is presented as an aid to visualization but does not represent any fit.



250 μm and the experiment was repeated using this higher surface area material. Under the same experimental conditions and reaction time, it was observed that approximately half of the polymer had disappeared; ¹H NMR analysis of the solution confirmed the presence of bisphenol A, indicating that the polymer was partially depolymerized. This suggests that the limiting step in the depolymerization of PC under these conditions is the mass transfer of catalyst and solvent into the polymer structure, so further effort was expended to optimize this process. Following the reports for the methoxide-promoted methanolysis of PC^{3,4}, we investigated the use of a cosolvent to increase the homogeneity of the reaction mixture and swell the residual solid polymer. Screening experiments were performed where approximately 35 mg of PC beads was placed into 1 mL of such solvents as dimethylformamide, 1,2-dichloroethane, chloroform, tetrahydrofuran, and dichloromethane at room temperature. While each of the solvents visibly showed swelling and softening of the polymer after 2 h, the beads placed in the chloroform were nearly completely dissolved, leaving a clear, yet viscous, solution. Subsequent experiments were performed to determine the effect on the rate of La^(III)-promoted methanolysis of **1e** as a function of methanol–chloroform mixtures (see Fig. 7). As the reaction rate is reduced with more chloroform, we chose 60:40 chloroform–methanol as a solvent mixture that represents a balance between the rate of reaction, reduced by a factor of ~9 relative to that in pure methanol at 25 °C, and dissolution of polymer in the solvent which essential for reaction.

A typical experiment comprised 200 mg of PC beads, crushed to 1–2 mm in size, and 2 mL of the 60:40 chloroform–methanol cosolvent mixture containing La(OTf)₃ and NaOMe (5 and 7.5 mmol dm⁻³, respectively), which was then heated to 100 °C for 10 min in a microwave reactor. Figure. S1 (see Supplementary material section) is an example of the ¹H NMR spectrum of a typical reaction mixture of this composition after depolymerization having 97% bisphenol A and 3% incompletely reacted PC or oligomers thereof. The effect of increasing PC loading was tested in this solvent system and the highest amount of PC accommodated in an experiment was 1000 mg in 2 mL of 60:40 chloroform–methanol catalyzed by La(OTf)₃:NaOMe (5:7.5 mmol dm⁻³). After heating at 100 °C for 30 min, the reaction reached approximately 84% completion as observed by ¹H NMR. This corresponds to 315 turnovers per equivalent of the catalyst.

Conclusions

The two metal ion containing catalytic systems efficiently promote the transesterification of a series of methyl aryl (**3**) and two methyl alkyl (**4**) carbonates. The computed mechanism of the re-

action of **1** with **3** and **4** involves the equilibrium formation of a transient complex between the metal catalyst (as its methoxide form) and substrate within which a two-step reaction leading to a set of intermediates with different lifetimes ensues. For aryl carbonates with LG whose conjugate acids have ^spK_a^{HOR'} values <16, the rate-limiting step is metal ion assisted delivery of a coordinated methoxide to the C=O of the transiently bound carbonate to form a tetrahedral intermediate with bidentate coordination to the metal ion. Breakdown of the intermediate is rapid and occurs with metal ion assistance of LG departure for the *p*-nitrophenoxy derivative and those with higher ^spK_a^{HOR'} values. Carbonates with -OAr LG having ^spK_a^{HOR'} values less than ~10 such as **3a** may decompose without metal ion assistance of LG departure.⁹ For methyl alkyl carbonates with LG whose conjugate acids have ^spK_a^{HOR'} values >18.13 (the ^spK_a of methanol), metal assisted departure of the LG is the rate-limiting step. Although we do not have reliable computational data²⁸ for the lanthanum catalytic system **2** due to the difficulties in dealing with the dimeric, highly charged catalyst, the general mechanism should be similar to that employed by **1**, but there is some question whether the La^(III)-promoted methanolysis of aryl carbonates does undergo a change in rate-limiting step from metal ion assisted nucleophilic attack to metal ion assisted departure of the LG.

It is interesting that these two systems have similar activities for all of the substrates; the maximum discrepancy is threefold, with **2** being slightly more active than **1** for methanolysis of substrates **3** having strong electron-withdrawing groups and **1** being twofold more reactive than **1** for the cleavage of **4b**. It is also interesting that, in terms of second-order rate constants for their catalytic reaction, both **1** and **2** have reactivities toward carbonates similar to that of methoxide. For the three carbonates where comparison can be made^{11a}, the *k*₂^{-OMe} rate constants for the methoxide reactions of **3b**, **3e**, and **4a** are 16.2, 0.47, and 0.0047 dm³ mol⁻¹ s⁻¹, respectively. These values are similar to the metal ion catalyzed rate constants in Table 1 for the substrates with good LG, but the metal-containing catalysts become progressively less reactive than methoxide as the carbonate LG becomes worse. The similarity of rate constant for the methoxide reaction and 1- and 2-promoted methanolysis of carbon esters has been seen before.^{5c} Thus, the catalytic benefit for metal-promoted carbonate and ester methanolysis is that maximum activity is reached at ^spH ~9, close to neutrality under catalytic conditions, while the methoxide-promoted reactions must be conducted at high base concentration under stoichiometric conditions.

The systems we report here may be effective for the larger scale decomposition of polycarbonates such as PC, although this reaction requires more severe conditions than where the mechanistic study was undertaken to circumvent the problem of penetration of the solution and catalyst into the polymer matrix. In one example, 1000 mg of PC in 2 mL of a 60:40 chloroform–methanol solution containing La(OTf)₃:NaOMe (5:7.5 mmol L⁻¹) at 100 °C for 30 min gave an 84% yield of bisphenol A, corresponding to >300 turnovers per molecule of catalyst. Further work may lead to preferred solvent systems having better catalyst and product recovery characteristics that enable solvent recycling.

Supplementary material

Supplementary material is available with the article through the journal Web site at <http://nrcresearchpress.com/doi/suppl/10.1139/cjc-2013-0270>. Electronic Supplementary information (ESI) available: tables of Cartesian coordinates for DFT-optimized structures, physical data for characterization of new carbonates **3f** and **3g**, ¹H NMR spectra for various decompositions of poly(bisphenol A) carbonate, and table of second-order rate constants corrected to 25 °C from ref. 11a and phenol ^spK_a values (adjusted to methanol

from aqueous values according to the formula given in ref. 5c used to prepare the Brønsted plots shown in Figs. 4 and 5.

Acknowledgements

The authors gratefully acknowledge the financial contributions of the Natural Sciences and Engineering Research Council of Canada and Queen's University for this research. In addition, D.S. acknowledges the NSERC Undergraduate Summer Research Awards program for support of his participation in this project and L.C. and S.G. acknowledge the support of the Summer Work Experience Program at Queen's University.

References

- Bozzano, G.; Dente, M.; De Rosso, R. In *Material Recycling-Trends and Perspectives*; Achilias, D., Ed.; ISBN 978-953-51-0327-1; InTech: Croatia, 2012; pp. 115-132, and references therein.
- Pinero, R.; Garcia, J.; Cocero, M. J. *Green Chem.* **2005**, *7*, 380. doi:10.1039/b500461f.
- Hu, L. C.; Oka, A.; Yamada, E. *Polymer* **1998**, *39*, 3841. doi:10.1016/S0032-3861(97)10298-1.
- Liu, F. S.; Li, Z.; Yu, S. T.; Cui, X.; Xie, C.-X.; Ge, X. P. *J. Polym. Environ.* **2009**, *17*, 208. doi:10.1007/s10924-009-0140-0.
- (a) Neverov, A. A.; McDonald, T.; Gibson, G.; Brown, R. S. *Can. J. Chem.* **2001**, *79* (11), 1704. doi:10.1139/v01-149; (b) Neverov, A. A.; Gibson, G.; Brown, R. S. *Inorg. Chem.* **2003**, *42*, 228. doi:10.1021/jc0203769; (c) Neverov, A. A.; Sunderland, N. E.; Brown, R. S. *Org. Biomol. Chem.* **2005**, *3*, 65. doi:10.1039/b414763d.
- (a) Lu, Z.-L.; Neverov, A. A.; Brown, R. S. *Org. Biomol. Chem.* **2005**, *3*, 3379. doi:10.1039/b508917d; (b) Neverov, A. A.; Brown, R. S. *Org. Biomol. Chem.* **2004**, *2*, 2245. doi:10.1039/b404740k; (c) Brown, R. S.; Lu, Z.-L.; Liu, C. T.; Tsang, W. Y.; Edwards, D. R.; Neverov, A. A. *J. Phys. Org. Chem.* **2010**, *23*, 1. doi:10.1002/poc.1584; (d) Brown, R. S.; Neverov, A. A. *Adv. Phys. Org. Chem.* **2008**, *42*, 271. doi:10.1016/S0065-3160(07)42006-8; (e) Liu, T.; Neverov, A. A.; Tsang, J. S. W.; Brown, R. S. *Org. Biomol. Chem.* **2005**, *3*, 1525. doi:10.1039/b502569a.
- We use the nomenclature recommended by the IUPAC, *Compendium of Analytical Nomenclature. Definitive Rules 1997*; 3rd ed.; Blackwell: Oxford, UK, 1998, for the designation of pH in non-aqueous solvents. The pH meter reading for an aqueous solution determined with an electrode calibrated with aqueous buffers is designated as ^wpH ; if the electrode is calibrated in water and the 'pH' of the neat buffered methanol solution then measured, the term ^spH is used; if the electrode is calibrated in the same solvent and the 'pH' reading is made, then the term ^ppH is used. In methanol, $^s\text{pH} - (-2.24) = ^p\text{pH}$. Since the autoprotolysis constant of methanol is $10^{-16.77}$, neutral ^ppH is 8.4. The methods for measurement of pH in methanol can be found in refs. 5, 6, and 17.
- Hatano, M.; Ishihara, K. *Chem. Comm.* **2013**, *49*, 1983. doi:10.1039/C2CC38204K, and references therein.
- Maxwell, C. I.; Neverov, A. A.; Mosey, N. J.; Brown, R. S. *J. Phys. Org. Chem.* Submitted for publication.
- Maxwell, C. I.; Liu, C. T.; Neverov, A. A.; Mosey, N. J.; Brown, R. S. *J. Phys. Org. Chem.* **2012**, *25*, 437. doi:10.1002/poc.1938.
- (a) Mitton, G.; Schowen, R. L.; Gresser, M.; Shapley, J. J. *Am. Chem. Soc.*, **1969**, *91*, 2036. doi:10.1021/ja01036a029; (b) Carpino, L. A.; Collins, D.; Gowecke, S.; Mayo, J.; Thatte, S. D.; Tibbetts, F. *Org. Syn.* **1964**, *44*, 22. doi:10.1002/0471264180.os044.08.
- Alder, R. W.; Mowlam, R. W.; Vachon, D. J.; Weisman, G. R. *J. Chem. Commun.* **1992**, 507. doi:10.1039/C39920000507.
- The term $^p\text{pK}_a$ refers to the pK_a of an acid measured in, and referenced to, an organic solvent, in this case methanol; see refs. 5, 6, and 7.
- (a) Tomasi, J.; Mennucci, B.; Cammi, R. *Chem. Rev.* **2005**, *105*, 2999. doi:10.1021/cr9904009; (b) Tomasi, J.; Mennucci, B.; Cancas, E. *THEOCHEM* **1999**, *464*, 211. doi:10.1016/S0166-1280(98)00553-3.
- (a) Hay, P. J.; Wadt, W. R. *J. Chem. Phys.* **1985**, *82*, 270. doi:10.1063/1.448799; (b) Wadt, W. R.; Hay, P. J. *J. Chem. Phys.* **1985**, *82*, 284. doi:10.1063/1.448800.
- Frisch, M. J.; Trucks, G. W.; Schlegel, H. B.; Scuseria, G. E.; Robb, M. A.; Cheeseman, J. R.; Scalmani, G.; Barone, V.; Mennucci, B.; Petersson, G. A.; Nakatsuji, H.; Caricato, M.; Li, X.; Hratchian, H. P.; Izmaylov, A. F.; Bloino, J.; Zheng, G.; Sonnenberg, J. L.; Hada, M.; Ehara, M.; Toyota, K.; Fukuda, R.; Hasegawa, J.; Ishida, M.; Nakajima, T.; Honda, Y.; Kitao, O.; Nakai, H.; Vreven, T.; Montgomery, J. A., Jr.; Peralta, J. E.; Ogliaro, F.; Bearpark, M.; Heyd, J. J.; Brothers, E.; Kudin, K. N.; Staroverov, V. N.; Kobayashi, R.; Normand, J.; Raghavachari, K.; Rendell, A.; Burant, J. C.; Iyengar, S. S.; Tomasi, J.; Cossi, M.; Rega, N.; Millam, J. M.; Klene, M.; Knox, J. E.; Cross, J. B.; Bakken, V.; Adamo, C.; Jaramillo, J.; Gomperts, R.; Stratmann, R. E.; Yazyev, O.; Austin, A. J.; Cammi, R.; Pomelli, C.; Ochterski, J. W.; Martin, R. L.; Morokuma, K.; Zakrzewski, V. G.; Voith, G. A.; Salvador, P.; Dannenberg, J. J.; Dapprich, S.; Daniels, A. D.; Farkas, Ö.; Foresman, J. B.; Ortiz, J. V.; Cioslowski, J.; Fox, D. J. *Gaussian 09*; Gaussian, Inc.: Wallingford, CT, 2009.
- Tsang, J. S.; Neverov, A. A.; Brown, R. S. *J. Am. Chem. Soc.* **2003**, *125*, 7602. doi:10.1021/ja034979a.
- (a) Taft, R. W., Jr. *J. Am. Chem. Soc.* **1952**, *74*, 2729. doi:10.1021/ja01131a010; (b) Taft, R. W., Jr. *J. Am. Chem. Soc.* **1953**, *75*, 4231. doi:10.1021/ja0113a027.
- These estimates are made on the basis of the measured ^ppH at half neutralization of the $[\text{12andN3}:\text{Zn(II)(HOCH}_2)_2]^{2+} \longleftrightarrow [\text{12aneN3}:\text{Zn(II)-(OCH}_2)_3]^+ + \text{H}^+$ system^{5c} and via potentiometric titration of La^{3+} in methanol; Gibson, G.; Neverov, A. A.; Brown, R. S. *Can. J. Chem.* **2003**, *81* (6), 495. doi:10.1139/v03-035.
- (a) Chaw, Z. S.; Fischer, A.; Happer, D. A. R. *J. Chem. Soc. (B)* **1971**, 1818. doi:10.1039/J29710001818; (b) Kirsch, J.; Clewell, A.; Simon, A. J. *Org. Chem. Soc. (B)* **1968**, *33*, 127. doi:10.1021/jo01265a023; (c) Humffray, A. A.; Ryan, J. J. *J. Chem. Soc. (B)* **1967**, 468. doi:10.1039/J29670000468.
- (a) Ryan, J. J.; Humffray, A. A. *J. Chem. Soc. (B)* **1966**, 842. doi:10.1039/J29660000842; (b) Bruice, T. C.; Mayahi, M. J. *Am. Chem. Soc.* **1960**, *82*, 3067. doi:10.1021/ja01497a023; (c) Kirsch, J. F.; Jencks, W. P. *J. Am. Chem. Soc.* **1964**, *86*, 837. doi:10.1021/ja01059a019.
- (a) Guthrie, J. P. *J. Am. Chem. Soc.* **1991**, *113*, 3941. doi:10.1021/ja00010a040.; (b) Stefanidis, D.; Jencks, W. P. *J. Am. Chem. Soc.* **1993**, *115*, 6045. doi:10.1021/ja00067a020.
- (a) Jencks, W. P. *Acc. Chem. Res.* **1980**, *13*, 161. doi:10.1021/ar50150a001; (b) Jencks, W. P. *Chem. Soc. Rev.* **1981**, *10*, 345. doi:10.1039/cs9811000345; (c) Williams, A. *Acc. Chem. Res.* **1989**, *22*, 387. doi:10.1021/ar00167a003.
- IUPAC. *Compendium of Chemical Terminology*, 2nd ed. (the "Gold Book"); Compiled by A. D. McNaught and A. Wilkinson; Blackwell Scientific Publications: Oxford, 1997; XML on-line corrected version: <http://goldbook.iupac.org> 2006, created by M. Nic, J. Jirat, B. Kosata; updates compiled by A. Jenkins. ISBN 0-9678550-9-8. doi:10.1351/goldbook.
- Babtie, A. C.; Lima, M. F.; Kirby, A. J.; Hollfelder, F. *Org. Biomol. Chem.* **2012**, *10*, 8095. doi:10.1039/c2ob25699a.
- Kim, S.-I.; Hwang, S.-J.; Jung, E.-M.; Um, I.-H. *Bull. Korean Chem. Soc.* **2010**, *31*, 2015. doi:10.5012/bkcs.2010.31.7.2015.
- Um, I.-H.; Seo, J. Y.; Kang, J. S.; An, J. S. *Bull. Chem. Soc. Jpn.* **2012**, *85*, 1007.
- Attempted calculations with $[\text{La}(\text{OCH}_2)_2]^{4+}$ were inconclusive due to presumed difficulties in providing good basis sets for the lanthanide ions and the large charges involved.
- The large suppression of translational and rotational degrees of freedom by bulk solvent is not captured, as substrates are treated as ideal gases. Bimolecular processes, such as this substrate-complex formation, have high entropic requirements and resulting free energies barriers tend to deviate from those calculated experimentally. See (a) Sumimoto, M.; Iwane, N.; Takahama, T.; Sakaki, S. *J. Am. Chem. Soc.* **2004**, *126*, 10457. doi:10.1021/ja040020r; (b) Tamura, H.; Yamasaki, H.; Sato, H.; Sakaki, S. *J. Am. Chem. Soc.* **2003**, *125*, 16114. doi:10.1021/ja0302937.